Carpathian Journal of Earth and Environmental Sciences, February 2012, Vol. 7, No. 1, p. 149 - 160

FLUID EVOLUTION AND ORE GENESIS OF THE QIANHE GOLD DEPOSITE, WESTERN HENAN PROVINCE, CENTRAL CHINA

Meijuan YAO[1], Junfeng SHEN[1] & Huapeng NIU[2]

[1]*State Key Laboratory of geological processes and mineral resources, China University of Geosciences, Beijing 100083, China. yaomeijuan1016@126.com*

[2]*China University of Petroleum, Beijing 102249, China*

Abstract: The Qianhe structure-controlled orogenic-mesothermal gold deposit is located in the Late Archean to Early Proterozoic metamorphosed volcanic and sedimentary rocks in the south margin of North China craton (NCC). Three stages of hydrothermal ore-forming processes are recognized, Early (E), Middle (M) and Late (L), characterized by coarse pyrite-quartz veins, fine pyrite-polymetallic sulfide veins and quartz-carbonate veins, respectively. Gold typically occurs as fracture-fillings associated with chalcopyrite and galena in M-stage. Fluid inclusions (FI) were examined in quartz from E-, M- and L-stage samples. FI petrography and microthermometric results suggest that three types of fluid inclusions are present at the deposit. Tm_{CO2} and Th_{CO2} in M-stage quartz range from -59.7 to -57.2°C and from 15.4 to 22.1°C, which are lower than those in E-stage quartz of ranging from -57.1 to -56.6°C and from 16.3 to 25.7°C. CO_2-rich inclusions have similar Tm_{CO2} and Th_{CO2} to those for CO_2-H_2O inclusions. CO_2-H_2O inclusions show salinities of 5.51 to 10.04 wt.% NaCl equivalent and Th of 242 to 336°C in E-stage quartz, and show salinities of 3.52 to 8.66 wt.% NaCl equivalent and Th of 213 to 240°C in M-stage quartz. Aqueous inclusions have a decreasing trend of salinities and Th from E-stage through M-stage to L-stage. Homogenization pressures of FI are estimated ranging from 367 to 872×10^5 Pa. The M-stage fluid has the lowest contents of ions (e.g., SO_4^{2-}, Cl^-, K^+) and (K+Na)/(Mg+Ca) but highest CO_2/H_2O ratios. The change in ore-forming fluids from K_2SO_4 type to NaCl type indicates the superposition of two hydrothermal mineralizing events. Together with the alkaline and reducing conditions, as indicated by decreased pH and increased Eh values, is most conducive to the deposition of polymetallic sulfides and native Au and electrum. Unlike in E-stage, FI in M- and L-stage quartz shows evidence of fluid immiscibility. The fact that most of gold is associated with M-stage quartz and sulfide but not with that of E-stage suggests that gold deposition occurs at the M-stage of fluid immiscibility. The sudden phase separation led to the deposition of large amounts of gold at the Qianhe deposit.

Key words: Fluid inclusion, Orogenic-type Au deposit, Ore genesis, Xiaoqinling, Qainhe,

1. INTRODUCTION

The Qianhe gold deposit in western Henan Province, about 1000 km southwest of Beijing, is located in Xiaoqingling gold district, which is the second largest gold producing area in China, with a geological reserve of 380 metric tons of gold, only exceeded by the Jiaodong gold Province (Li et al., 1996; Qiu et al., 2002).

More than 100 gold deposits and occurrences have now been discovered, including several deposits with >20 t Au (Nie, 1997). Results from a few studies of the gold metallogeny (e.g. Qiyugou, Shanggong, Wenyu, Kangshan, Hongzhuang, et al. Fig. 1b) have been published in the western literature (Jiang et al., 1999; Jiang & Zhu 1999; Jiang, 2000; Chen et al., 2006, 2008; Fan et al., 2009). As one of the big scale gold deposits in Xiaoqingling gold district, the Qianhe deposit has a resource of about 1Moz of Au metal with ore grades averaging 7.87g/ton Au (Ba et al., 2006).

Ag and Te can be recovered as by-products, but their reserves and grades have not been reported (Mao et al., 2002). The Qianhe was only referred in those studies, but has not been reported in detail on English journals. Previous studies in Chinese (Yuan & Pei, 1997; Li et al., 1999; Ba et al., 2006; Cao et al., 2007, 2008, 2009; Yao et al., 2008) were mainly focused on geological survey and deep prospecting, with only a few studies on fluid nature and its evolution.

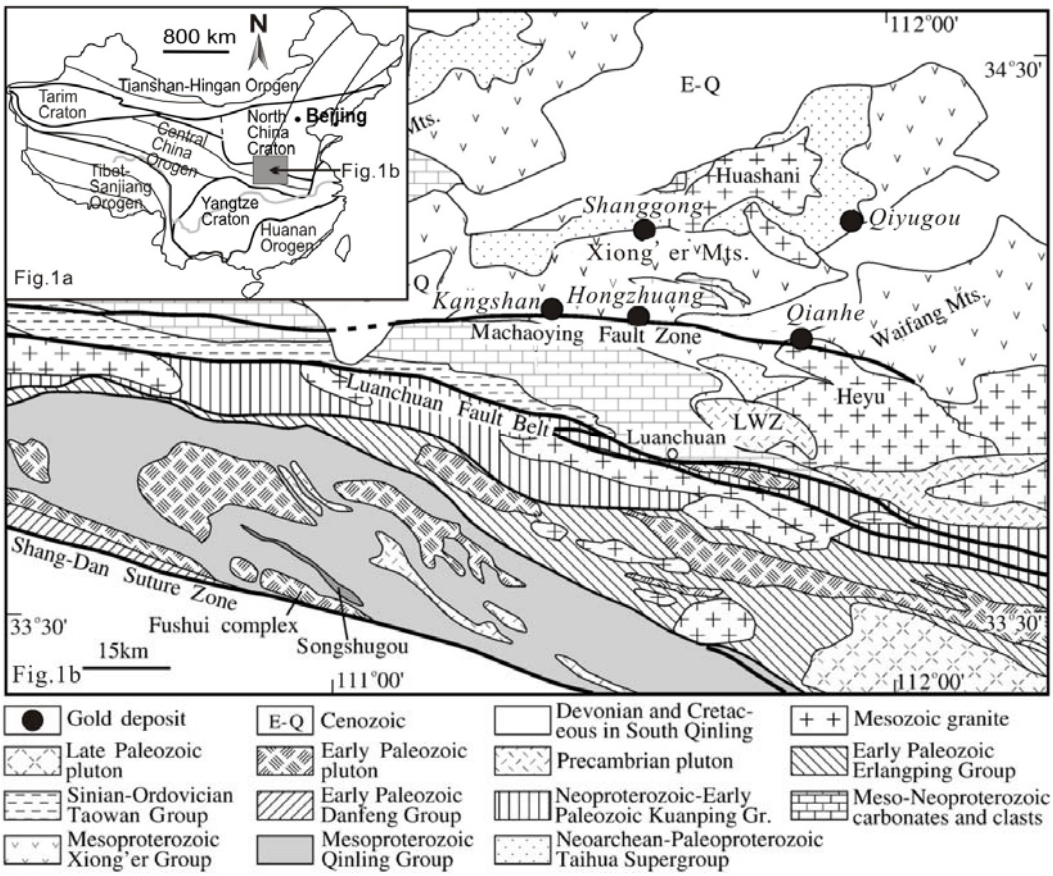

Figure 1. Location of the Qianhe gold deposit. Fig. 1a The major tectonic domains of China (after Chen et al., 2006); Fig. 1b A simplified geological map of the western Henan province along the southern margin of the NCC (modified after Henan Bureau of Geology and Mineral Resources, 1989; Lu et al., 2003; Han et al., 2009). LWZ—Longwangzhuang pluton.

Because the research on fluid inclusion is ideal for discussion on genesis of hydrothermal gold deposits, in this paper, preliminary fluid inclusion measurements on the Qianhe deposits will be reported, and then summarize the results of ore geology and fluid studies to discuss the ore genesis in the context of metallogenic complexity of Xiaoqinling gold district.

2. GEOLOGICAL SETTING

2.1. Regional geology

The Qianhe deposit is hosted in andesite and dacite of the Xiong'er Group in the Xiong'er Terrane, Henan Province, China (Fig. 1). The Xiong'er Terrane is one of the Precambrian terranes at the southern margin of the North China craton (NCC), and is the result of a complex tectonic evolution related to the Mesozoic continental collision between the NCC and the Yangtze cratons (Hu et al., 1988; Chen & Fu, 1992; Chen & Zhao, 1997). Gold deposits and occurrences in this region are exposed in a 270-km-long by 45- to 100-km-wide area of the southern margin of the NCC.

The main lithostratigraphic units of the Xiong'er Terrane are the Taihua Group (basement) and the Xiong'er Group (cover). Their original rocks of Taihua group are intermediate-basic volcanic clastic rocks and sedimentary rocks, and they have U-Pb zircon ages of 2.8-2.6 Ga, with xenocrystic zircons as old as 2.9 Ga (Hu et al., 1988; Kroner et al., 1988; Xue et al., 1996). The rocks has been repeatedly metamorphosed and migmatitized, resulting in metamorphic rocks of amphibolite facies such as plagioclase amphibolite, biotite plagioclase gneiss, quartzite, marble and various migmatites. The Xiong'er Group, with 4 to 9 km-thick sequence and an inferred areal extent of about 60,000 km^2 (Zhao et al., 2002) unconformably overlies the Taihua Group and is covered by clastic rocks of the Late Proterozoic Taowan (or Xiaoshan) Group. Rocks of the Xiong'er Group include basaltic andesite, dacite and rhyolite, with minor sedimentary intercalations and pyroclastic units. These volcanic rocks have Rb-Sr and U-Pb zircon ages of 1.8-1.4 Ga (Ren & Li 1996), and range between lower greenschist and amphibolite metamorphic facies (Hacker et al. 1996).

More than 20 Mesozoic granitoids with Mesozoic in age are exposed in the region, such as the 784 km^2 Heyu and 130 km^2 Huashan intrusion, which yield LA ICP-MS zircon U-Pb weight average ages of 133.8±1.1Ma and 134.5±1.5Ma, respectively (Guo et al., 2009). Numerous northeast-trending faults are spatially control the Au deposits of the Xiong'er Terrane (Fig. 1b). Take the Machaoying fault zone as an example, it trends WNW along the southern margin of the NCC and is immediately north of the North Qinling Orogenic Belt (NQOB). This fault controls the distribution of the Mesoproterozoic volcanic rocks of the Xiong'er Group, the Guandaokou carbonate sequences, and Mesozoic gold and molybdenum deposits (Hu et al., 1988; Liu et al., 1998; Chen et al., 2004, 2009). Dating of K-feldspar from a quartz–K-feldspar vein in the Machaoying fault zone yields a ^{40}Ar-^{39}Ar plateau age of 119.5±0.7 Ma (Han et al., 2009), which overlaps the age of widespread gold and molybdenum mineralization in the region.

2.2. Deposit geology

The Qianhe deposit is located at east end of the Machaoying fault (Fig. 1b). The deposit contains three parts with total 15 ore bodies. All the orebodies are contained in high strain zones and are distributed in a EW-trending belt, about 3800 m long, 100 m wide (Fig. 2). Most veins strike N-E and dip 58°~76° (Fig. 3). The No. IV vein system, the largest vein in the mine, can be traced for 830m at least alone strike and varies from 0.5 to 14.97m in thickness. The mine workings have been extended to a depth of over 500 m (Fig. 4). Repeated pinching and swelling of the veins along strike and dip direction is common. Ore shoots are preferentially located in swells resulting from a change in the strike and dip of the veins.

Orebodies are usually within silicified zones that have brecciated, mylonitic and banded structures and form stockworks, disseminated veinlets or massive veins. The hydrothermal processes responsible for the Qainhe mineralization resulted in a distinctive lateral zoning, which from the orebodies to the country rocks includes (Fig. 5): ore bodies (Au content of ca. 7.87g/t); argillization zone; breccia zone; schistositized zone; joint development zone; cataclastic rock zone; propylite zone; unaltered country rock of the Xiong'er Group (Au content of ca. 0.7 ppb; Chen & Fu, 1992). Ore minerals in vein systems are mainly native gold, electrum, pyrite, chalcopyrite, sphalerite, galena, with minor pyrrhotite, magnetite, bornite, hematite. Gangue minerals are dominated by quartz, biotite, calcite, feldspar, epidote, fluorite, chlorite and kaolinite.

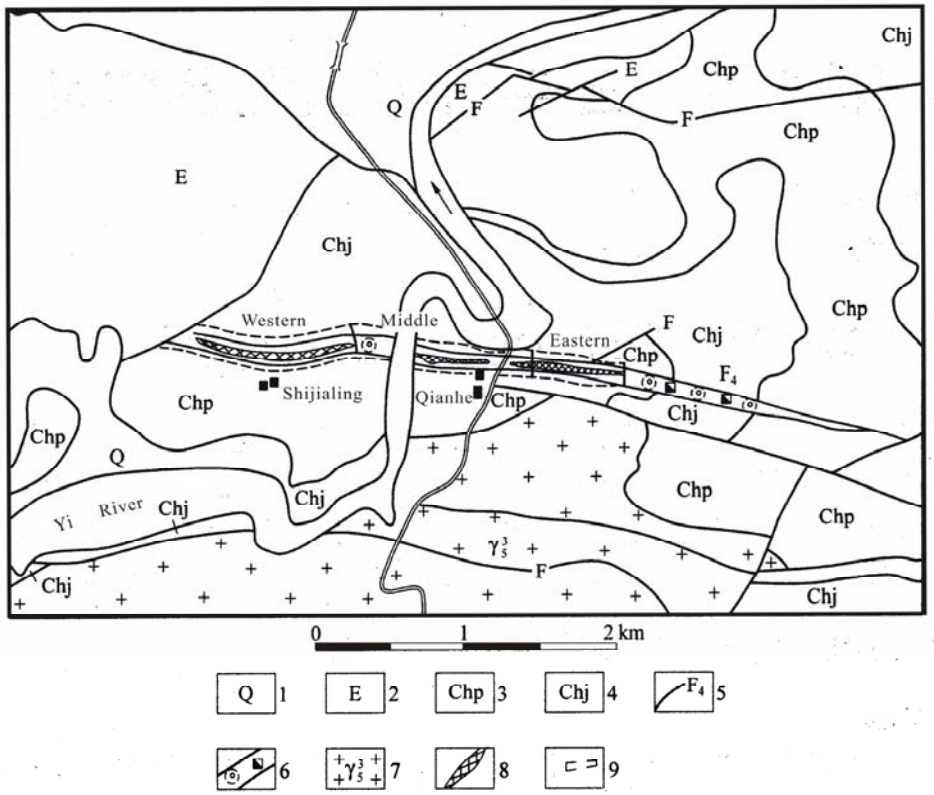

Figure 2. Simplified geologic map of the Qianhe gold deposit showing the distribution of ore bodies in the fault belts (after Li et al., 1999; Zhang et al., 2006). 1-Quaternary; 2-Tertiary; 3-Majiahe foramtion of Xiong'er group; 4-Jidanping foramtion of Xiong'er group; 5-Faults and Faults □6-the fracture alteration zone; 7-late Yanshanian porphyritic adamellite; 8-Gold orebodies; 9-Ore block.

Three mineralizing stages of veining have been identified on the basis of textural, mineralogical, and crosscutting relationships observed in hand specimens and thin sections. They include a pyrite-quartz stage (E-stage), a quartz-sulfide stage (M-stage) and a quartz-carbonate stage (L). The E-stage is characterized by compact and massive milky white quartz (95%) and coarse-grained euhedral pyrite (5%) with minor sericite, albite, hematite, etc. M-stage typify fine stockworks filled the brecciated E-stage coarse-grained milky quartz veins. The stockworks are composed of pyrite, galena, sphalerite, chalcopyrite, minor native elements (Au, Ag). M-stage gangue minerals include quartz, chlorite, sericite, epidote. The L-stage is dominated by quartz-carbonate veinlets, locally associated with fluorite, bornite, clay minerals. The L-stage veinlets penetrate mineralized fracture zones and country rocks. According the mineral assemblages in different stages, we can deduce a paragenetic sequence of the major ore and alteration minerals as shown in Figure 6. From the microscope observation, most Au grains are hosted in M-stage minerals such as pyrite, sphalerite, galena and chalcopyrite. The fineness of native Au ranges from 786.6 to 956.4.

3. FI PETROGRAPHY

Doubly polished thin sections were prepared from eight representative samples of the quartz from early to late stage, those of which were collected from the underground mining levels between the present surface, at 560m and a depth of 220m. FI at the Qianhe deposit have a variety of shapes (mainly round, elongate, or negative crystal, and, less commonly, irregular shapes). From the petrographic study, three different types of fluid inclusions were identified on the basis of the number of phases and liquid to vapor ratios at room temperature. Isolated inclusions, those forming irregular three-dimensional groups within grains or along growth plane were classified as primary. Inclusions occurring along planes crosscutting grain boundaries were considered secondary inclusions (Roedder, 1984).

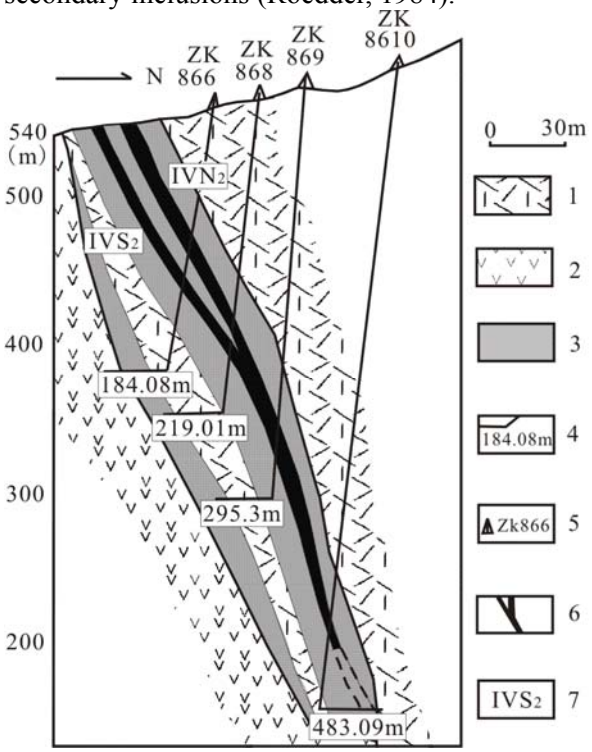

Figure 3 A profile along No. 87 exploration line, showing the vertical relationship between oredodies and altered wall rocks. 1-rhyolite; 2-andesite; 3-mylonitization; 4-depth of drill hole; 5-location of drill hole and its numbering; 6-gold ore bodies; 7-ore bodies numbering.

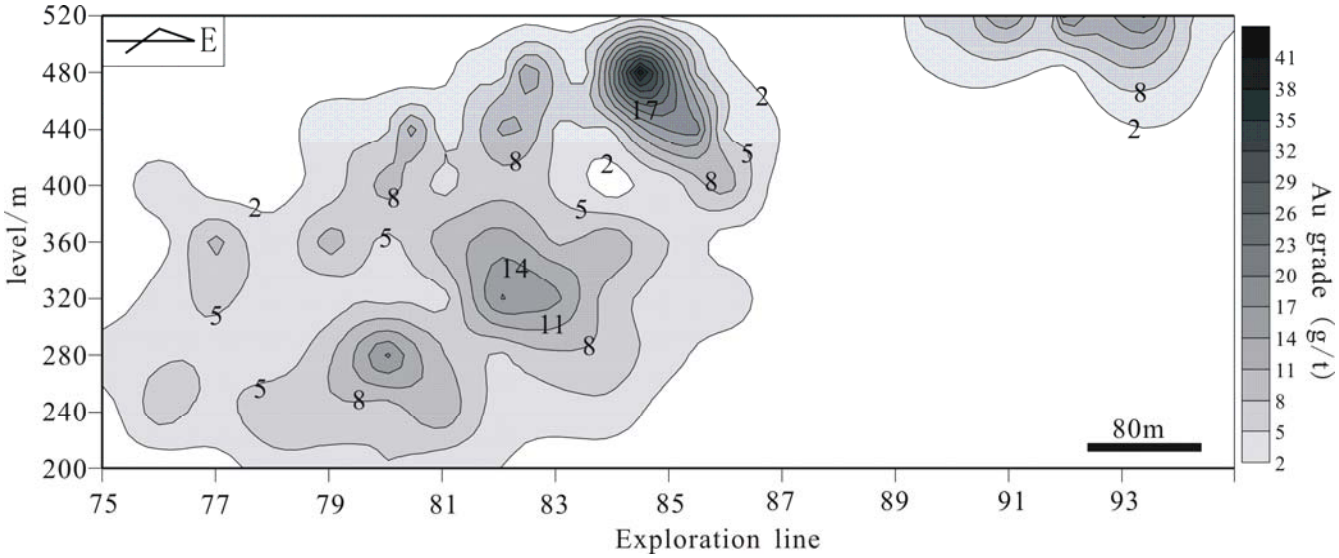

Figure 4. The contour for Au grade of No.IV orebody of the Qianhe gold deposit

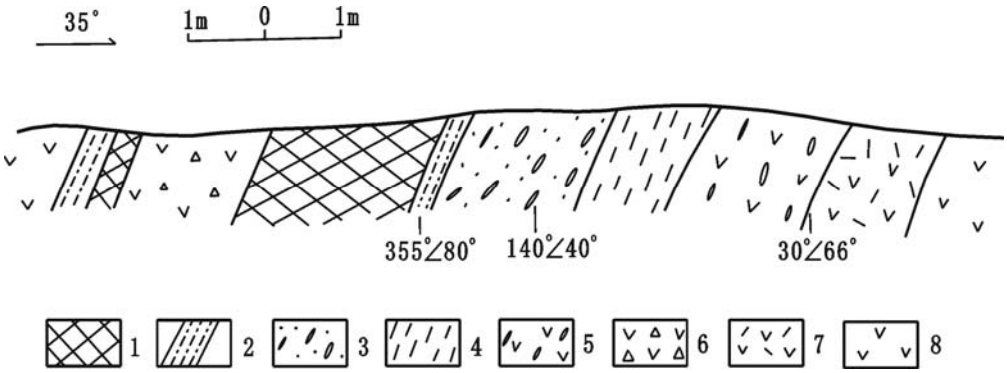

Figure 5. A profile of No. IV fault hosting ore bodies. 1-ore bodies; 2-argillization zone; 3-breccia zone; 4-schistositized zone; 5-joint development zone; 6-cataclastic rock zone; 7-propylite zone; 8-andesite.

Mineral	Py-qtz stage (Early stage I)	Qtz-sulfide stage (Middle stage II)	Carbonate stage (Late stage III)
K-feldspar	▬▬	▬ ▬ ▬	
Biotite	▬▬		
Rutile	▬ ▬ ▬		
Albite	▬ ▬		
Chlorite	▬▬	▬ ▬ ▬	▬▬
Epidote	▬▬	▬ ▬	▬▬
Sericite	▬ ▬ ▬	▬▬	
Quartz	▬▬	▬▬	▬ ▬ ▬
Pyrrhotite		▬ ▬ ▬	
Pyrite	▬ ▬ ▬ ▬	▬▬	▬ ▬ ▬ ▬
Native gold		▬▬	
Electrum		▬ ▬	
Galena		▬ ▬ ▬ ▬	
Chalcopyrite		▬ ▬	
Sphalerite		▬ ▬	
Actinolite			▬ ▬
Fluorite			▬ ▬ ▬
Calcite		▬ ▬ ▬	▬▬
Bornite			▬ ▬ ▬

Figure 6. Paragenetic sequence of hydrothermal minerals of the Qianhe deposit

3.1. CO_2-rich inclusions

CO_2-rich inclusions have negative crystal shapes and occur in E-stage and M-stage quartz. In general, inclusions of this type consist of a single or two (liquid CO_2 +vapor CO_2) phases at room temperature (Fig. 7a,b,c,e). They appear as one phase due to CO_2 homogenizing to liquid CO_2 in E-stage quartz and as two phases in M-stage quartz. They range from 4 to12 μm and coexist with CO_2-H_2O inclusions or occur as clusters and are interpreted as primary or pseudosecondary in origin. Locally, they also occur with CO_2-H_2O inclusions.

3.2. CO_2-H_2O inclusions

CO_2-H_2O inclusions in quartz have similar sizes typically between 5 and 20 μm. They exhibit negative crystal shapes, but can also be irregular shapes. The total CO_2 volumes, varies from 10 to 80 % of the total inclusion volume. Most CO_2-H_2O inclusions appear as two phases in E-stage quartz (Fig. 7e,f,h), but as three phases in M-quartz at room temperature (Fig. 7a,b,c,d). These inclusions occur as irregular, three-dimensional clusters in E-stage quartz, whereas as isolated inclusions in M-stage quartz. All CO_2-H_2O inclusions are generally confined to individual quartz grains and are considered primary in origin.

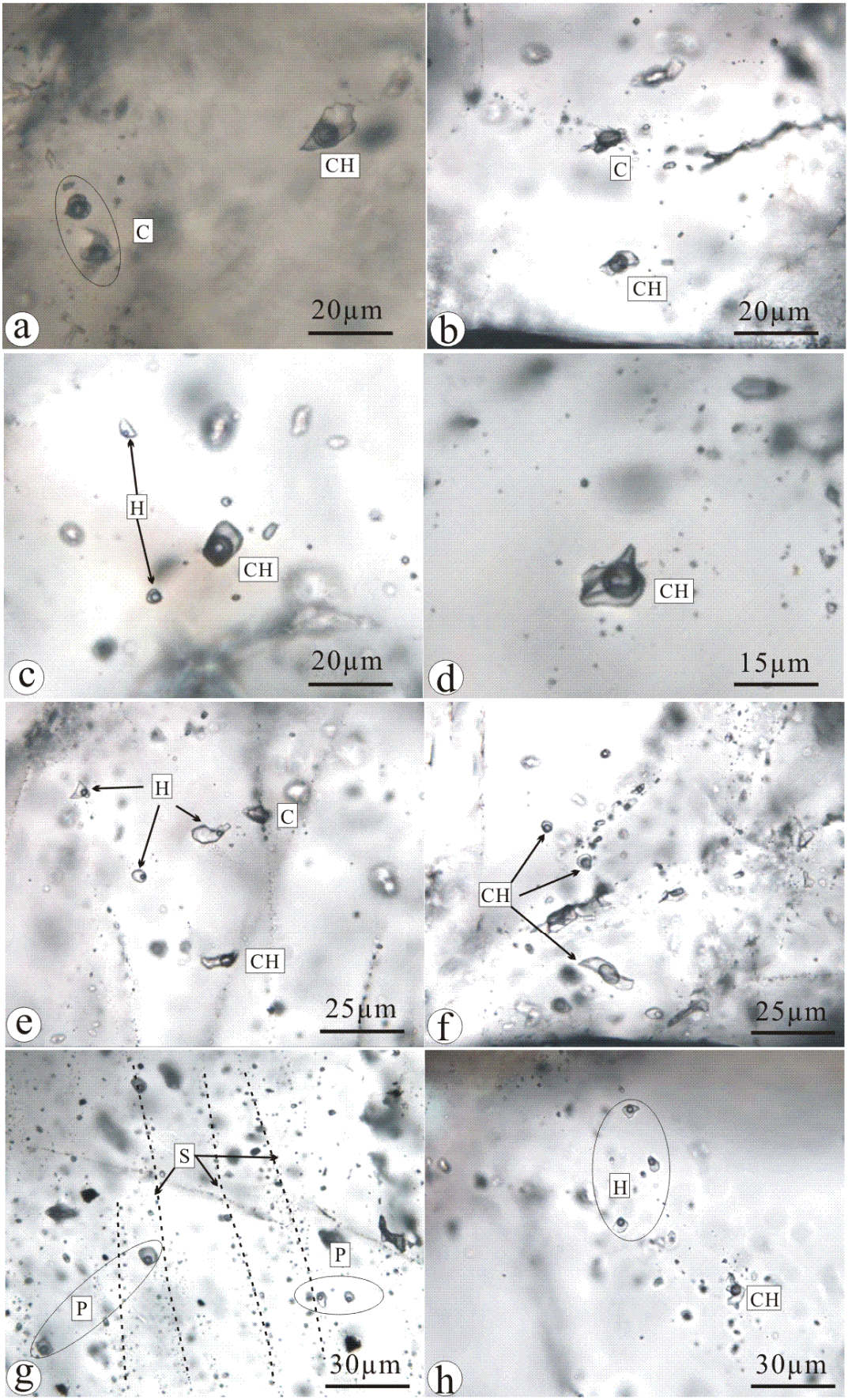

Figure 7. Photomicrographs of fluid inclusion types from quartz of the Qianhe deposit. CH= CO_2-H_2O inclusions, C= CO_2-rich inclusions; H= Aqueous inclusions; P=primary; S=secondary.

3.3. Aqueous inclusions

This type is characterized by a vapor bubble in an aqueous liquid at room temperature, are found in most L-stage quartz. Generally, some inclusions along microfractures cutting quartz grains are relatively small (<10μm) with a degree of filling of 0.90, as trails along healed fractures and crosscut the CO_2-H_2O inclusions (Fig. 7e). They are undoubtedly secondary in origin. Aqueous inclusions as three-dimensional clusters and isolated individuals coexisting with CO_2-H_2O or CO_2-rich inclusions have irregular or round shapes and range from 8 to 18μm (Fig. 7e,g,h). They are interpreted as primary in origin and usually have a lower filling degree than secondary inclusions.

4. FI MICROTHERMOMETRY

The microthermometric study was carried out in the Fluid Inclusion Laboratory at the Chinese University of Geosciences (Beijing).

Microthermometric measurements were made on doubly polished thin sections (about 0.2mm thick) using Linkam equipment (THMS 600 freezing-heating stage, TMS94 temperature control system and LNP2 freezing control system) and a coupled image analysis system to observe phase changes. The equipment was calibrated using a set of synthetic inclusions, distributed by Fluid Inc., USA. The temperature measurements can be reproduced within ±0.2°C in the range -60 to +100°C, within ±0.5 to 2°C in the range -60 to -120°C, within ±3°C in the range -120 to -180°C, and about ±2°C for temperatures above +100°C.

4.1. FI in E-stage quartz

The CO_2-H_2O inclusions homogenize between 242 and 336°C, with the majority of analyses between 235 and 305°C. Melting temperatures of CO_2 (Tm_{CO2}) in CO_2-H_2O inclusions are slightly lower than -56.6°C (Fig. 8), suggesting less contamination of the CO_2 with other volatiles. (Cioaca, 2011). The clathrate melting temperatures (Tm_{clath}) obtained from analyses range from 4.3-7.1°C. According to Collins (1979), these Tm_{clath} correspond to salinity of 5.51-10.04 equivalent wt% NaCl. The CO_2 homogenization temperatures (Th_{CO2}) of E-stage range from 16.3 to 25.7°C, clustering around 19°C. CO_2-rich inclusions have similar Tm_{CO2} and Th_{CO2} to those for CO_2-H_2O inclusions.

Homogenization temperatures (Th) of primary aqueous inclusions range from 243 to 332°C with an average of 275°C (Fig. 9). Melting temperatures of ice (Tm,ice) of aqueous inclusions range from -9.1 to -4.5°C, correspondingly range from 7.17 to 12.96 wt% NaCl equivalent according to the equation of (Bodnar, 1993).

4.2. FI in M-stage quartz

The majority of CO_2-H_2O inclusions have CO_2 homogenizing to liquid. The CO_2-H_2O inclusions homogenize within a narrow range from 213 and 240°C. Tm_{CO2}, Tm_{clath}, and Th_{CO2} are shown in Fig. 8. The melting temperatures of CO_2 significantly lower than -56.6°C, suggesting much contamination of the CO_2 with other volatiles, such as Ar, N_2, H_2S. The clathrate melting temperatures obtained from analyses range from 5.2~8.2°C, corresponding the salinities of ranging between 3.52 and 8.66 wt% NaCl equivalent. Th of primary aqueous inclusions ranges from 207 to 246°C with an average of 229°C. Tm_{ice} of primary aqueous inclusions ranges from -7.6 to -3.4°C, correspondingly range from 5.56 to 11.22 wt% NaCl equivalent.

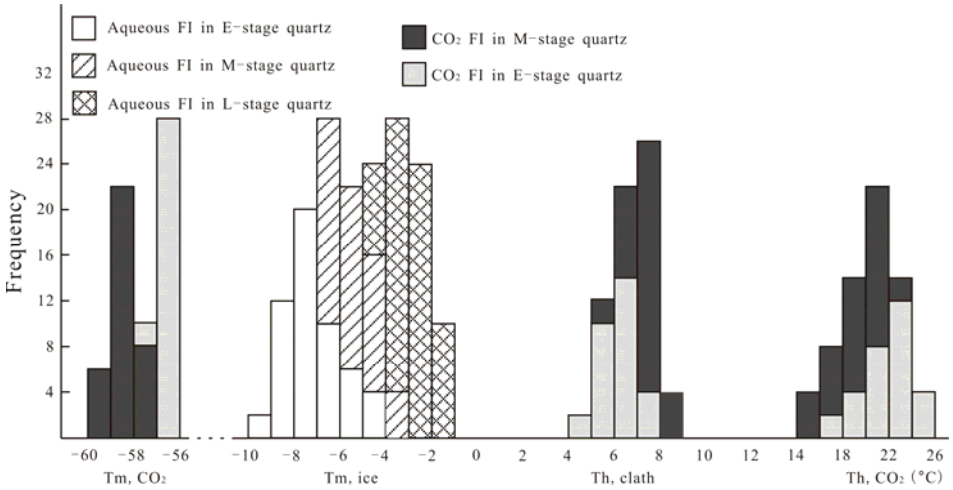

Figure 8. Frequency vs. Tm-CO_2, Tm-ice, Tm-clath and Th-CO_2 histogram from fluid inclusion microthermometric data.

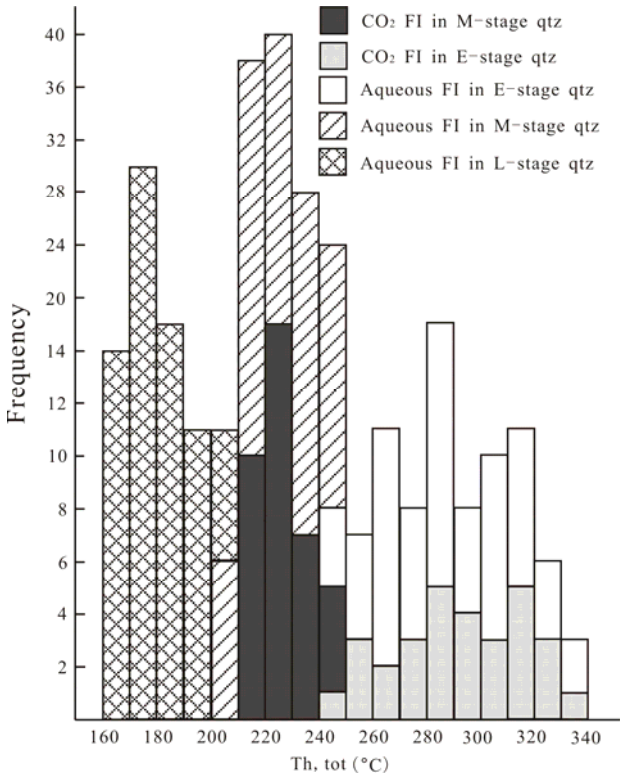

Figure 9. Frequency vs. Th-tot histogram from fluid inclusion microthermometric data.

4.3. FI in L-stage quartz

CO_2-H_2O and CO_2-rich inclusions are very rare in this stage quartz. All the aqueous inclusions homogenize to liquid and range from 165-210°C, with the majority of analyses smaller than 200°C. Tm_{ice} of primary aqueous inclusions ranges from -4.7 to -1.8°C, correspondingly range from 7.45 to 3.06 wt% NaCl equivalent.

According to NaCl-H_2O reference table of Liu & Shen (1999), using final homogenization temperatures and salinities of aqueous inclusions in the above three stage quartz, the resulting densities of the aqueous (ρH_2O) phase range from 0.68-0.76 g/cm^3, 0.80-0.89 g/cm^3 and 0.90-0.94 g/cm^3, and the homogenization pressures range from 576.88-896.55×10^{5}Pa, 502.86-710.57×10^{5}Pa, 367.01-518.78×10^{5}Pa in E-stage, M-stage and L-stage quartz, respectively.

5. CHEMICAL COMPOSITION OF FI

Analysis of bulk chemical composition of fluid inclusions was carried out at the IGGCAS by HIC-6A ion chromatograph and RG202 quadrupole mass spectrometer. The analyzing procedure is as follows. The dried washed sample, weighing 50 mg, was put in a clean quartz tube and was heated to 100°C. Then, the valve was turned on and the gas pipe was vacuumed. When the pressure in the quartz tube was just less than the value of 6×10^{-6} Pa, the burst stove was heated to 260, 320, and 500°C in steps. The instrument and working conditions of gas analysis are as follows: instrument is HIC-6A ion chromatograph made by Japan SHIMADZU; columns are Shim-pack IC-A3 and Shim-pack IC-C3; mobile phase; flow is Anio 1.2 mL/min and ion 1.0 mL/min; temperature is 40 °C; detector is CCD-6A 3.2 μs/cmFS; and injection volume is 50μL. Reproducibility for gas components is about ±5‰ (1σ). The instrument and working condition of liquid components are as follows: instrument is RG202 quadrupole mass spectrometer made by Japan ULVAC; SME voltage is -1.22 V; ionization way is EI; ionizing energy is 50 eV and measure speed is 50 ms/amu. Reproducibility for liquid components is about ±5‰ (1σ). Analysis results of fluid inclusion components are shown in Table 1.

The concentration of CO_2 ranges from 1.577 to 15.456 mol %. There is a large range for N_2 from under detection limit to 5.202 mol %. The CH_4 content of ranging from 0.03435-1.183 mol % is variable and consistently less than N_2. The Ar content in all of the samples is small. The C_2H_6 content, approximately equal to CH_4, is ranging from 0.02048-7.112 mol %.

All samples contain minimum H_2S ranging from 0.00221-0.277 mol %. The CO_2/H_2O ratio increases drastically in M-stage, showing that CO_2 might be enriched in the fluid system. CO_2 is an important buffer in the gold ore-fluid system (Phillips & Evans, 2004). CO_2, H_2S and other volatile enriched in fluid system resulting from boiling could make the fluids oversaturated and more reduced, so cause the following two reaction, $H_2O+CO_2 \rightarrow H_2CO_3 \rightarrow H^+ + HCO_3^- \rightarrow 2H^+ + CO_3^{2-}$, and $H^+ + S^{2-} \rightarrow HS^-$. This could result in the rapid deposition of sulfides and native elements.

The composition of the inclusion fluids is given in Table 1. Mg^{2+} and Ca^{2+} are about one order of magnitude less than Na^+ and K^+. The high contents of Ca^{2+} (4.23μg/g) and low Mg^{2+} in L-stage solution possibly resulted in calcite precipitation but no ankerite. The content of SO_4^{2-} represents the total content of various species of sulfur due to oxidization during the analyses.

Among the three mineralization stages, the M-stage fluid has the highest contents of SO_4^{2-} and K^+, which are conducive to $[Au(HS)_2]^-$ transportation (Phillips & Evans, 2004) and sulfidation and potassium alteration. The concentration of Cl^- ranges from 0.435 × 10^{-6} to 27 × 10^{-6}, which is a few less than SO_4^{2-} content ranging from 4.17 × 10^{-6} to 33 × 10^{-6}.

Table1. Chemical composition and physicochemical parameters of ore-forming fluids of the Qianhe gold deposit

Sample No.	20081	28075	24081	40081	20082	24076	48084
Ore stage	E	E	M	M	M	M	L
H_2O	97.572	95.797	88.57	88.78	80.21	80.443	97
CH_4	0.361	0.359	0.07834	0.111	0.114	1.183	0.03435
N_2	-	-	3.838	4.169	5.202	-	1.105
C_2H_6	0.457	0.358	0.0614	0.0932	0.1082	7.112	0.02048
H_2S	0.033	0.251	0.01199	0.01203	0.02094	0.277	0.00221
Ar	0	0.054	0.02884	0.04341	0.02406	0.361	0.01329
CO_2	1.577	3.181	7.572	6.393	15.456	10.624	1.756
CO_2/H_2O	0.0162	0.0332	0.0855	0.0720	0.1927	0.1321	0.0181
Cl^-	5.97	2.57	2.00	9.15	2.15	0.435	27
SO_4^{2-}	26.4	8.58	10.388	6.78	33	9.51	4.17
Na^+	7.98	3	2.589	5.55	5.13	0.185	21
K^+	0.6	0.528	0.231	0.405	1.81	-	0.405
Mg^{2+}	0.177	0.072	-	-	-	-	0
Ca^{2+}	2.53	0.801	0.899	2.22	-	-	4.23
$\sum M^+$	11.287	4.401	3.719	8.175	6.94	0.185	25.635
$\sum M^-$	32.37	11.15	12.388	15.93	35.15	9.945	31.17
K/Na	0.0752	0.1760	0.0892	0.0730	0.3528	-	0.0193
KN/MC	3.1696	4.0412	3.1368	2.6824	-	-	5.0603
$lgfO_2$	-31.73	-36.23	-31.5	-36.02	-36.58	-35.97	-42.42
$lgfCH_4$	-0.41	-0.448	-1.081	-0.959	-0.952	0.072	-1.506
$lgfH_2O$	1.143	0.947	1.2	0.902	0.878	0.94	0.831
$lgfCO_2$	0.099	0.339	0.788	0.639	1.021	0.876	0.029
$lgfH_2S$	-1.777	-0.971	-2.183	-2.295	-2.048	-0.904	-3.065
pH	5.689	5.3	4.837	4.675	4.429	4.597	4.483
Eh	-0.395	-0.36	-0.318	-0.304	-0.281	-0.297	-0.286

Note: gas components in mol%, liquid components in μg/g, Eh value in mv; "-" blow detection limit; $\sum M^+$ and $\sum M^-$ represent total contents of cations and anions, respectively. KN/MC=(K+Na)/(Mg+Ca). $lgfO_2$ is the fugacity of oxygen, hereinafter.

The Cl^- content in the M- stages fluids is lower than that in the E- and L-stage fluids. This is consistent with the appearance of fluorite coexisting with quartz at the L-stage. The high contents of Cl^- in E-stage fluid are interpreted as one of the most important ligands to coordinate with Au under high temperature~400°C (Ulrich et al., 1999; Ulrich, 2003; Stefansson & Seward, 2003). The values of total content of cations (ΣM+) and anions (ΣM-), and total content of ions (ΣM±) in the M-stage fluids are lower than those in the E- and L-stages fluids, suggesting that the ore metals (Au and Ag) tend to precipitate simultaneously with those ions from the M-stage fluids.

The pH value of the composite of the fluids at E-stage was measured about 5.3~5.7. This is slightly higher than those for M-stage (4.4 to 4.8) and L-stage (4.5) and therefore less acidic. Less acidic usually means higher anion (e.g. S^{2-} and HCO_3^- or CO_3^{2-}) activities, which is conducive to mineral precipitation. Experimental studies show (Widler & Seward, 2002) that low pH can support higher aqueous activity of hydrosulfide-Au and promotes the reduction of Au^+ to metallic Au^0. Meanwhile, the Eh value for the composite of E-stage fluids is about -0.40~-0.36, which is lower than those for the M-stage (-0.28~-0.32) and L-stage (-0.286), thereby indicating more reduced conditions in the M-stage. This lowest Eh value helps the reduction of Au^+, Ag^+, Cu^{2+}, Pb^{2+}, Zn^{2+} to the native state.

6. FLUID EVOLUTIONS AND GOLD MINERALIZATION

The fluids preserved in M-stage quartz are represented by coexistent primary CO_2-rich, CO_2-H_2O and aqueous inclusions. These inclusions are interpreted to the result from phase separation of a parent homogeneous NaCl-H_2O-CO_2 fluid during M-stage. The fluids preserved in E-stage quartz are

represented by CO_2-rich and aqueous inclusions, and the fluid in L-stage quartz are represented by aqueous inclusions. The aqueous inclusions are thought to have a different origin as the CO_2-rich inclusions. The CO_2-H_2O inclusions in M-stage quartz have lower both Th and Th_{CO2} than those of E-stage quartz. It suggests NaCl-H_2O-CO_2 fluid system evolved from higher CO_2 content, higher trapping pressure and temperature and higher Th_{CO2} to lower CO_2 content, lower trapping pressure and temperature and lower Th_{CO2}, and indicates the CO_2-H_2O inclusions in E- and M-stage may have a common origin. In contrast to the decreasing trapping pressure and temperature and CO_2 content with time, the salinity also did vary much in the NaCl-H_2O-CO_2 fluid system from E-stage through M-stage to L-stage. In the L-stage quartz, the fluid was characterized by lower Th, salinity and lower or non-CO_2 aqueous inclusions.

Fluid immiscibility is commonly cited to be responsible for gold precipitation in orogenic-mesothermal Au deposits (Bowers, 1991; Mao et al., 2003; Xu et al., 2008). Observed features suggesting CO_2 and H_2O immiscibility at the Qianhe deposit are in agreement with the criteria of Roedder (1984) and Lu et al. (2004). CO_2-rich, CO_2-H_2O and aqueous inclusions with different degrees of filling appear to be coeval, and their homogenization temperatures are similar are different even they have different homogenization model. It indicates trapping of a fluid that was either undergoing phase separation (boiling) or formed by simultaneous separation of immiscible brine and vapour from a magma cooling.

Similar to the case of the Qianhe deposit, Mao et al. (2003) noted that gold is precipitated during main stage of gold mineralization in the Dongping deposit, north margin of NCC. They suggested that the combination of CO_2 enrich, increase in Eh and the decreased pH, T and P of the fluid will lead to decreased solubilities for a variety of phases, resulting in the precipitation of phases such as quartz and sulfide. The decrease in pH leads to a decrease in solubility of gold due to the decreased abundance of HS^- relative to H_2S (Widler & Seward, 2002), so native Au is deposited during the M-stage. The temperature and pressure of E-stage fluids are much higher than that of M-stage fluid, which is much higher than that of L-stage fluid. In particular, the CO_2 content in the fluids drastically increases in M-stage. This fluid evolution suggests that fluid immiscibility is accompanied by decrease in P and T, but increase in CO_2 content. The fact that most of gold is associated with the M-stage quartz and sulfide suggests that gold deposition occurs at the M-stage of fluid immiscibility. The sudden phase separation led to the deposition of large amounts of gold at the Qianhe deposit.

ACKNOWLEDGEMENTS

This research is funded by National Natural Science Foundation Major Research Plan Key Support Project (Grant No. 90914002), and the 111 Project under the Ministry of Education and the State Administration of Foreign Experts Affairs, China (Grant No. B07011). We are very grateful to an anonymous referee who reviewed our manuscript with very constructive comments that greatly improved it.

REFERENCES

Ba, A.M., Ma, H.Y., Zhang, S.S. & Tian, X.Q., 2006. *Ore characteristics and ore-searching direction of Qianhe gold mine in Singxian county, Henan province*. Contribution to geology and mineral resources, 21(2), 100-114 (in Chinese with English abstract).

Bodnar, R.J., 1993. *Revised equation and table for determining the freezing point depression of H_2O-NaCl solutions*. Geochimica et cosmochimica acta, 57, 683–684.

Bowers, T.S., 1991. *The deposition of gold and other metals: Pressure-induced fluid immiscibility and associated stable isotope signatures*. Geochimica et cosmochimica acta, 55, 2417–2434.

Cao, Y., Li, S.R., Shen, J.F., Yao, M.J., Li, Q.K. & Mao, F.L., 2007. *Relation between the characteristics of magnetic susceptibilities of altered rocks and gold mineralization in the Qianhe gold deposit, Henan*. Geology in China, 34(6), 1082-1090 (in Chinese with English abstract).

Cao, Y., Li, S.R., Shen, J.F., Yao, M.J., Li, Q.K. & Mao, F.L., 2008. *Application of portable infrared mineral analyzer (PIMA) in the Qainhe gold mine, Henan province*. Geology and Prospecting, 44(2), 82-86 (in Chinese with English abstract).

Cao, Y., Li, S.R., Shen, J.F. & Yao, M.J., 2009. *Hydrothermai alteration geochemistry of the Qianhe gold deposit in western Henan Province*. Geology in China, 36(1), 156-165 (in Chinese with English abstract).

Chen, Y.J. & Fu, S.G., 1992. *Gold Mineralization in West Henan, China*. China Seismological Press, Beijing, pp. 234 (in Chinese with English abstract).

Chen, Y.J. & Zhao, Y.C., 1997. *Geochemical characteristics and evolution of REE in the Early Precambrian sediments: evidences from the southern margin of the North China craton*. Episodes, 20, 109-116.

Chen, Y.J., Pirajno, F. & Sui, Y.H., 2004. *Isotope geochemistry of the Tieluping silver-lead deposit, Henan, China: a case study of orogenic silver-dominated deposits and related tectonic setting*. Mineralium Deposita, 39, 560–575.

Chen, Y.J., Pirajno, F., Qi J.P., Li, J. & Wang, H.H.,

2006. *Ore Geology, Fluid Geochemistry and Genesis of the Shanggong Gold Deposit, Eastern Qinling Orogen, China*. Resource Geology, 56(2), 99-116.

Chen, Y.J., Pirajno, F. & Qi, J.P., 2008. *The Shanggong gold deposit, Eastern Qinling Orogen, China: Isotope geochemistry and implications for ore genesis*. Journal of Asian Earth Sciences, 33, 252-266.

Chen, Y.J., Pirajno, F., Li, N., Guo, D.S. & Lai, Y., 2009. *Isotope systematics and fluid inclusion studies of the Qiyugou breccia pipe-hosted gold deposit, Qinling Orogen, Henan province, China: Implications for ore genesis*. Ore Geology Reviews, 35, 245-261.

Cioaca, M.E., 2011. *Fluid evolution in the Bolcana ore deposit, Metaliferi Mountains (Romania)*. Carpathian Journal of Earth and Environmental Sciences, 6, 215-224.

Collins, P.L.F., 1979. *Gas hydrates in CO_2-bearing fluid inclusions and the use of freezing data for estimation of salinity*. Economic Geology, 74, 1435-1444.

Fan, H.G., Hu, F.F., Wilde, S.A., Yang, K.F. & Jin, C.W., 2009. *The Qiyugou gold-bearing breccia pipes, Xiong'ershan region, central China: fluid-inclusion and stable-isotope evidence for an origin from magmatic fluids*. International Geology Review, 53, 25-45

Guo, B., Zhu, L.M., Li, B., Gong, H.J. & Wang, J.Q., 2009. *Zircon U-Pb age and Hf isotope composition of the Huashan and Heyu granite plutons at the southern margin of North China craton: Implication for geodynamic setting*. Acta Petrologica Sinica, 25(2), 265-281

Hacker, B.R., Wang, X., Eide, E.A. & Ratschbacher, L., 1996. *The Qinling–Dabie ultra-high-pressure collisional orogen*. In: Yin A, HarrisonM (eds) The tectonic evolutionof Asia. Cambridge University Press, Cambridge, pp. 345-370.

Han, Y.G., Zhang, S.H., Pirajno, F., Wang, Y. & Zhang, Y.H., 2009. *New ^{40}Ar–^{39}Ar age constraints on the deformation along the Machaoying fault zone: Implications for Early Cambrian tectonism in the North China Craton*. Gondwana Research, 16, 255-263.

Henan Bureau of Geology and Mineral Resources, 1989. Regional Geology of Henan Province. Geological Publishing House, Beijing. pp. 772 (in Chinese with English abstract).

Hu, S.X., Lin, Q.L., Chen, Z.M. & Li, S.M., 1988. *Geology and Metallogeny of the Collision Belt between the North and the South China Plates*. Nanjing Univ. Press, Nanjing, pp. 558 (in Chinese with English abstract).

Jiang, N., Xu, J. & Song, M., 1999. *Fluid inclusion characteristics of mesothermal gold deposits in the Xiaoqinling district, Shaanxi and Henan Provinces, People's Republic of China*. Miner Deposita, 34, 150-162.

Jiang, N. & Zhu, Y., 1999. *Geology and genesis of orogenic gold deposits, Xiaoqinling district, southeastern China*. International Geology Review, 41, 816-826.

Jiang, N., 2000. *Hydrothermal Fluid Evolution Associated with Gold Mineralization at the Wenyu Mine, Xiaoqinling District, China*. Resource Geology, 50, 103-112

Kroner, A., Compston, W., Zhang G.W., Guo, A.L. & Todt, W., 1988. *Age and tectonic setting of late Archean greenstone-gneiss terrain in Henan Province, China, as revealed by single-grain zircon dating*. Geology, 16, 211- 215.

Li, L., Qing, M. & Chen, X., 1999. *Geochemical features of Qianhe gold deposit, Henan*. Gold Geology, 5(3), 75-80 (in Chinese with English abstract).

Li, S., Chu, L., Su, Z., Huang, J., Wang, X. & Yue, Z., 1996. *Geology and Metallogenic Prognosis of Gold Deposits in Xiaoqinling District, China*. Geological Press, Beijing, pp.250. (in Chinese).

Liu, H.Y., Hu, S.X. & Zhou, S.Z., 1998. *A study of rock-controlling and ore-controlling role of the Machaoying fault in western Henan*. Mineral Deposits, 17, 70-81 (in Chinese with English abstract).

Liu, B. & Shen, K., 1999. *Thermo-dynamics of fluid inclusions*. Geological Publishing House, Beijing, pp. 66–118, and pp. 171–233 (in Chinese).

Lu, H.Z., Fan, H.R., Ni, P., Ou, G.X., Shen, K. & Zhang, W.H., 2004. *Fluid inclusions*. Science Press, Beijing, pp. 1-487 (in Chinese).

Lu, S.N., Li, H.K., Chen, Z.H., Hao, G.J., Zhou, H.Y., Guo, J.J., Niu, G.H. & Xiang, Z.Q., 2003. *Meso-Neoproterozoic geological evolution in the Qinling Orogeny and its response to the supercontinental events of Rodinia*. Geological Publishing House, Beijing. pp.194 (in Chinese with English abstract).

Mao, J.W., Goldfarb, R.J., Zhang, Z.W., Xu, W.Y., Qiu, Y.M. & Deng, J., 2002. *Gold deposits in the Xiaoqinling–Xiong'ershan region, Qinling Mountains, central China*. Mineralium Deposita, 37, 306-325.

Mao, J.W., Li, Y.Q., Goldfarb, R. & He, Y., 2003. *Fluid Inclusion and Noble Gas Studies of the Dongping Gold Deposit, Hebei Province, China: A Mantle Connection for Mineralization?* Economic Geology, 98, 517-534.

Nie, F.J., 1997. *An overview of the gold resources of China*. International Geology Review, 39, 55-81.

Phillips, G.N. & Evans, K.A., 2004. *The role of CO_2 in the formation of gold deposits*. Nature, 429, 860-863.

Qiu, Y.M., Groves, D.I., McNaughton, N.J., Wang, L.G. & Zhou, T.H., 2002. *Nature, age, and tectonic setting of granitoid-hosted, orogenic gold deposits of the Jiaodong Peninsula, eastern North China craton, China*. Mineralium Deposita, 37, 283-305.

Ren, F.G. & Li, W.M., 1996. *Ore-forming geological conditions and models for ore searching and ore evolution of gold deposit in Xiong'ershan–Xiaoshan areas*. Geological

Publishing House, Beijing, pp. 1-130 (in Chinese).

Roedder, E., 1984. *Fluid Inclusions*. Mineral. Soc. Amer., Reviews in Mineralogy, 12, pp.644.

Stefansson, A. & Seward, T.M., 2003. *Stability of chloride-gold(I) complexes in aqueous solutions from 300 to 600°C and from 500 to 1800 bar*. Geochimica et cosmochimica acta, 67, 4559-4576.

Ulrich, T., Gunther, D. & Heinrich, C.A., 1999. *Au concentrations of magmatic brines and the metal budget of porphyry copper deposits*. Nature, 399, 676–679.

Ulrich, T., 2003. *Applications of quantitative single fluid inclusion analysis using laser ablation ICPMS*. Earth Sci. Frontiers, 10, 379-393.

Widler, A.M. & Seward, T.M., 2002. *The adsorption of Au(I) hydrosulphide complexes by iron sulphide surfaces*. Geochimica et cosmochimica acta, 66, 383-402.

Xu, J.H., Ding, R.F., Xie, Y.L., Zhong, C.H. & Shan, L.H., 2008. *The source of hydrothermal fluids for the Sarekoubu gold deposit in the southern Altai, Xinjiang, China: Evidence from fluid inclusions and geochemistry*. Journal of Asian Earth Sciences, 32, 247-258.

Xue, F., Kroner, A., Reischmann T., Lerch, F., 1996. *Paleozoic pre- and post-collision calc-alkaline magmatism in the Qinling orogenic belt, central China, as documented by zircon ages on granitoid rocks*. Journal of the Geological Society (London), 153, 406-417.

Yao, M.J., Shen, J.F., Li, S.R., Cao, Y. & Liu, X.Y., 2008. *Thermoelectric and thermal decrepitation characteristics of pyrite in the Qianhe gold deposit, Songxian County, Henan, China, and their relationships with gold mineralization*. Geological Bulletin of China, 27(5), 649-656 (in Chinese with English abstract).

Yuan, H.G. & Pei, Y.H., 1997. *The characteristics of the wall rock and host rock of the orthophyric tectonic altered rock-type gold deposit in Qianhe area*. Henan Geology, 15(1), 24-28 (in Chinese with English abstract).

Zhang, Y.H., Zhang, S.H., Han, Y.G. & Zhang, H.J., 2006. *Strike-slip features of the Machaoying fault zone and its evolution in the Huaxiong terrane, Southern North China craton*. Journal of Jilin University (Earth Science Edition), 36(2), 169-176 (in Chinese with English abstract).

Zhao T.P., Zhou M.F., Zhai M. & Xia, B., 2002. *Paleoproterozoic rift-related volcanism of the Xiong'er Group, North China Craton: implications for the breakup of Columbia*. International Geology Review, 44, 336-351.

Received at: 05. 07. 2011
Revised at: 29. 09. 2011
Accepted for publication at:28. 10. 2011
Published online at: 31. 10. 2011